



UNIVERSITY OF LEEDS

This is a repository copy of *Terahertz emission mechanism and laser excitation position dependence of nano-grating electrode photomixers*.

White Rose Research Online URL for this paper:
<http://eprints.whiterose.ac.uk/110178/>

Version: Accepted Version

Proceedings Paper:

Mohandas, RA, Freeman, JR, Rosamond, MC et al. (8 more authors) (2016) Terahertz emission mechanism and laser excitation position dependence of nano-grating electrode photomixers. In: 2016 41st International Conference on Infrared, Millimeter, and Terahertz waves (IRMMW-THz). 41st International Conference on Infrared, Millimeter, and Terahertz waves (IRMMW-THz), 25-30 Sep 2016, Copenhagen, Denmark. IEEE . ISBN 9781467384858

<https://doi.org/10.1109/IRMMW-THz.2016.7758713>

© 2016 IEEE. Personal use of this material is permitted. Permission from IEEE must be obtained for all other uses, in any current or future media, including reprinting/republishing this material for advertising or promotional purposes, creating new collective works, for resale or redistribution to servers or lists, or reuse of any copyrighted component of this work in other works.

Reuse

Unless indicated otherwise, fulltext items are protected by copyright with all rights reserved. The copyright exception in section 29 of the Copyright, Designs and Patents Act 1988 allows the making of a single copy solely for the purpose of non-commercial research or private study within the limits of fair dealing. The publisher or other rights-holder may allow further reproduction and re-use of this version - refer to the White Rose Research Online record for this item. Where records identify the publisher as the copyright holder, users can verify any specific terms of use on the publisher's website.

Takedown

If you consider content in White Rose Research Online to be in breach of UK law, please notify us by emailing eprints@whiterose.ac.uk including the URL of the record and the reason for the withdrawal request.



eprints@whiterose.ac.uk
<https://eprints.whiterose.ac.uk/>

Terahertz emission mechanism and laser excitation position dependence of nano-grating electrode photomixers

Reshma A. Mohandas^a, Joshua R. Freeman^a, Mark C. Rosamond^a, Lalitha Ponnampalam^b, Alwyn J. Seeds^b, P. J. Canard^c, M. J. Robertson^c, D. G. Moodie^c, A. Giles Davies^a, Edmund H. Linfield^a and Paul Dean^a

^{a)} Institute of Microwaves & Photonics, University of Leeds, Leeds, LS2 9JT, United Kingdom

^{b)} University College London, London, WC1E 6BT, United Kingdom

^{c)} CIP Technologies, Aadastral Park, Martlesham Heath, Ipswich, Suffolk, IP5 3RE, United Kingdom

Abstract— The emission mechanism of continuous wave (CW) terahertz (THz) photomixers that make use of nanostructured gratings (NSGs) is studied. Two different photomixer designs, based on a single-sided NSG and a double-sided NSG, embedded in the same antenna design and fabricated on an Fe doped InGaAsP substrate, are characterized with ~ 1550 nm excitation. They are shown to exhibit similar performance in terms of spectral bandwidth and emitted power. The emission is mapped in terms of the laser excitation position, from which the emission mechanism is assigned to an enhanced optical electric field at the tips of the NSGs.

I. INTRODUCTION

THERE have been several reports of enhanced THz emission from photomixers incorporating nanostructured electrodes both in pulsed [1] and CW operation [2, 3]. In particular, plasmonic nanostructure emitters based on NSGs have been reported to result in better optical coupling to the semiconductor substrate as well as decreased carrier transit times (and therefore lifetimes) owing to the excitation of surface plasmons [1] bound to the metal-semiconductor interface. This second effect could reduce the reliance on semiconductor materials with short carrier lifetimes for the development of wide-bandwidth THz emitters. The present study focuses on the generation mechanism behind nanostructure grating (NSG) electrodes and the applicability of these structures to CW THz photomixers operating at telecommunications wavelengths.

II. RESULTS

Two different photomixer designs, based on a single-sided nanostructured (SSN) grating and a double-sided nanostructured (DSN) grating were fabricated on Indium Gallium Arsenide Phosphide ($\text{In}_{0.70}\text{Ga}_{0.30}\text{As}_{0.87}\text{P}_{0.13}$) substrates grown by MOCVD with an Fe doping concentration of $4 \times 10^{16} \text{ cm}^{-3}$. The fabrication procedure was the same as described in ref [4]. The NSGs consisted of 100-nm-wide metal lines with a 200 nm pitch, and are identical to those of references [1] and [2], which are reported to provide enhanced absorption for both 780 nm and 1550 nm optical radiation. The SSN device incorporated the grating only on one side of the active region with the other electrode left unstructured. The DSN design incorporated gratings on both electrodes. Both nanostructured designs had an active region of $19 \mu\text{m} \times 19 \mu\text{m}$, and were coupled to a two-turn logarithmic spiral antenna (see Fig. 1). A bias of 1 V at a frequency of 7.6 kHz and 25% duty cycle was applied across the NSG arm of the SSN and DSN emitters for characterization.

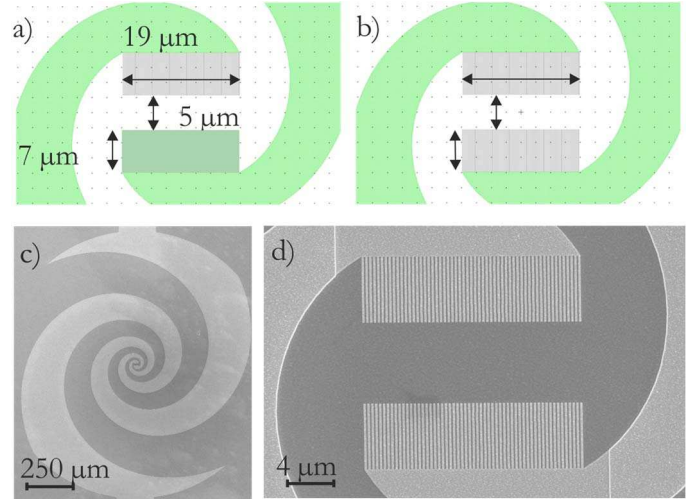


Fig 1: Schematic of the (a) SSN and (b) DSN emitters. SEM images of the fabricated (c) log-spiral antenna and the active region of the (b) DSN emitter fabricated on the Fe:InGaAsP wafer.

The devices were characterized using a pair of tunable CW distributed Bragg reflector lasers with emission tunable between 1534–1565 nm. One laser was kept at a fixed wavelength and the other laser was electrically tuned. The output from the fibre-coupled lasers was combined and split with a 2×2 fibre splitter. The output from one fibre was collimated through a half-wave plate then focused with an aspheric lens onto the emitter with an incident power of 10 mW. The generated THz radiation was collimated using a 3.0-mm diameter hyper-hemispherical silicon lens, attached to the backside of the substrate, and a parabolic mirror. Radiation was then focused to the detector using a second parabolic mirror. The second fibre output was connected to a fibre-coupled InGaAs coherent receiver purchased from TOPTICA Photonics. The second parabolic mirror and detector were placed on a mechanical delay line to enable phase control and ensure the optimum path difference between the emitter and detector. The current generated in the detector was amplified using a FEMTO trans-impedance amplifier with a gain of $10^7 \Omega$ and measured using a lock-in amplifier [4].

Figure 2 shows the measured spectral bandwidth obtained from the SSN and DSN emitter. Both emitters were found to exhibit similar performance in terms of bandwidth (~ 2 THz) and output power (~ 1 nW at 1 THz) compared to the same antenna design with a more conventional interdigitated finger active region. To gain an insight into the mechanism for THz emission from the SSN and DSN emitters, mapping of the THz emission as a function of laser excitation position was carried out. The laser beam was focused to a spot size of ~ 6 – $7 \mu\text{m}$ using

an Olympus 20 \times microscope objective. The sample was raster scanned in the X-Y plane (perpendicular to the excitation direction) with the laser spot remaining stationary. It was confirmed that this small movement of the sample did not affect the collection efficiency; this is because the silicon lens attached to the back of the substrate has a diameter twice that of the antenna structure.

Figures 3 (a)–(d) show the mapping of the THz emission as a function of laser excitation position, obtained at 510 GHz from the SSN and DSN emitters with different electrodes biased. From the data, we can see that for both designs the maximum

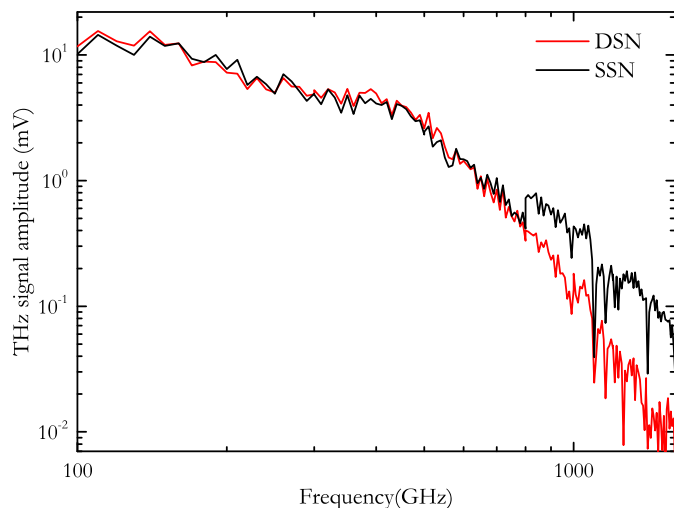


Fig 2: THz signal amplitude as a function of heterodyne frequency for the SSN and DSN emitter with the NSG arm biased at 1 V.

THz radiation is obtained when the laser excitation spot is positioned in the gap between the two electrodes. There is also no significant emission when the excitation spot is positioned at the center of one of the NSGs. These measurements indicate that the THz generation in these devices appears to be associated with the tips of the nano-grating electrodes rather than the center of the grating structure. When the bias direction is switched, the DSN emitter maintained the same maximum power level, and a small change in the position of the maximum was observed. For the SSN emitter, reversing the bias caused a significant reduction in power (more than half), but the excitation position corresponding to the highest emitted power did not change significantly. Mapping of the laser excitation of the emitters for higher frequencies showed similar behavior, but with a reduced total signal. The laser excitation was horizontally polarized for these measurements; polarizing the excitation vertically (i.e. parallel to the applied electric field in the gap, shown in Fig 3 (e) and (f)) reduced the observed signal by 70 % and 30% for SSN and DSN emitters, respectively. The decrease in output power is due to the NSGs acting as a wire-grid polarizer. The smaller change in the SSN emitter confirms this effect, as there is only one NSG for that emitter.

In summary, this data shows that the THz generation in these devices appears to be associated with the tips of the nano-grating electrodes rather than the center of the grating structure. The sharp tips can cause an enhancement in the absorption of the laser radiation because of the concentration of optical electric field at the sharp corners. As a result, photons experience a higher absorption in the vicinity of the metal tips

causing an enhanced emission when exciting in this region. In the case of SSN emitters, when the plane metal electrode is positively biased no enhanced output power is observed because there are no sharp tips present.

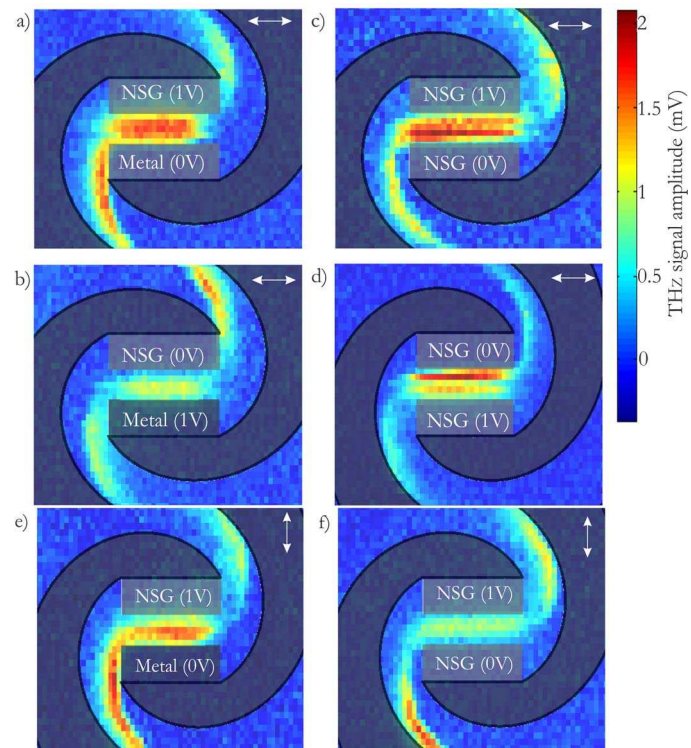


Fig 3: Raster scanned image to show the THz amplitude as a function of the laser exciting position at 1V bias. Data for the SSN emitter is shown with (a) the NSG biased and (b) the metal electrode biased. Data for the DSN emitter is shown with (c) the first NSG biased and (d) the second NSG biased. Data in (a)–(d) is for horizontal polarization. (e) and (f) show the map for vertical polarizations for the SSN and DSN, respectively.

III. ACKNOWLEDGEMENTS

This work was supported by the Engineering and Physical Sciences Research Council (EPSRC) grant COTS (EP/J017671/1). We also acknowledge support from the ERC programme TOSCA; the Royal Society and Wolfson Foundation (AGD); and EPSRC Fellowships (PD, EP/J002356/1).

IV. REFERENCES

- [1] C. W. Berry, N. Wang, M. R. Hashemi, M. Unlu, and M. Jarrahi, "Significant performance enhancement in photoconductive terahertz optoelectronics by incorporating plasmonic contact electrodes," *Nat Commun*, vol. 4, p. 1622, 2013.
- [2] C. W. Berry, M. R. Hashemi, S. Preu, H. Lu, A. C. Gossard, and M. Jarrahi, "High power terahertz generation using 1550 nm plasmonic photomixers," *Applied Physics Letters*, vol. 105, p. 011121, 2014.
- [3] TanotoH, J. H. Teng, Q. Y. Wu, SunM, Z. N. Chen, S. A. Maier, WangB, C. C. Chum, G. Y. Si, A. J. Danner, and S. J. Chua, "Greatly enhanced continuous-wave terahertz emission by nano-electrodes in a photoconductive photomixer," *Nat Photon*, vol. 6, pp. 121-126, 2012.
- [4] R. A. Mohandas, J. R. Freeman, M. C. Rosamond, O. Hatem, S. Chowdhury, L. Ponnampalam, M. Fice, A. J. Seeds, P. J. Cannard, M. J. Robertson, D. G. Moodie, J. E. Cunningham, A. G. Davies, E. H. Linfield, and P. Dean, "Generation of continuous wave terahertz frequency radiation from metal-organic chemical vapour deposition grown Fe-doped InGaAs and InGaAsP," *Journal of Applied Physics*, vol. 119, p. 153103, 2016.